Characterization of the intercalate $C_{60}(CO_2)_x$ by powder neutron diffraction

M. James,* S. J. Kennedy, M. M. Elcombe, and G. E. Gadd
Australian Nuclear Science and Technology Organisation, Private Mail Bag 1, Menai NSW 2234, Australia
(Received 29 June 1998)

The intercalate compound $C_{60}(CO_2)_x$ has been synthesized by hot isostatically pressing C_{60} under 170 MPa of CO_2 and 350 °C. Neutron powder diffraction studies conducted on $C_{60}(CO_2)_x$ between room temperature and 5 K have been analyzed using Rietveld techniques and reveal a structural transition between a high-temperature ($\gtrsim$250 K) face-centered cubic phase [$Fm\bar{3}m$, $a=14.224(2)$ Å (293 K)] and a low-temperature ($\lesssim$150 K) monoclinic phase [$P2_1/n$, $a=9.7438(9)$ Å, $b=9.7473(9)$ Å, $c=14.6121(11)$ Å, $\beta=90.390(6)°$ (5 K)]. The CO_2 molecules occupy the octahedral interstices between the C_{60} molecules and are oriented along the body diagonal of the high-temperature phase. In the low-temperature phase they are tilted slightly away from the *c* axis so as to place the oxygen atoms adjacent to the center of a pentagonal face on the C_{60} molecules. [S0163-1829(98)05545-3]

INTRODUCTION

Over the past few years the trapping of gases interstitially in fullerite materials has received considerable attention, including the intercalation of atomic rare gases (He, Ne, Ar, Kr, and Xe) (Refs. 1–5) and molecular gases (H_2 and O_2).[6–9] The intercalation of CO into solid C_{60} has also recently been reported.[10]

Solid C_{60} is composed of C_{60} molecules held together in a face-centered cubic (fcc) array by van der Waals forces, which at room temperature are insufficient to prevent free rotation of the C_{60} molecules. Cooling of the solid sees the domination of van der Waals forces over the thermal energy of the C_{60} molecules and orientational ordering occurs at ~249 K producing a structural transition from fcc ($Fm\bar{3}m$) to simple cubic (sc) ($Pa\bar{3}$).[11] An isostructural phase transition occurs for $C_{60}O_2$ (Ref. 9) and $(CO)_xC_{60}$ (Ref. 10) as well as for the rare gas intercalate phases R_xC_{60} with transition temperatures that decrease with increasing intercalate radius: 250 K (R=Ar, $x=1.0$), 240 K (Kr, $x=0.84$), 210 K (Xe, $x=0.66$).[3]

Based on a cell constant of C_{60} of approximately 14.19 Å the van der Waals radius of cubic close-packed C_{60} molecules is 5.01 Å and the lattice contains one interstitial octahedral site of minimum radius 2.06 Å and two tetrahedral sites of minimum radius 1.13 Å per C_{60} molecule.[6,12] Given a C–O bond length of 1.165 Å (Ref. 13) and a van der Waals radius for O of 1.52 Å,[14] it is expected that CO_2, like the rare gases, CO and O_2, should only occupy the octahedral interstitial site. In addition, given the size of the CO_2 molecules, it is unlikely that they would be able to freely tumble in the octahedral interstices as has been suggested for O_2 molecules with a van der Waals radius of 2.00 Å.[6]

EXPERIMENT

Synthesis

Two grams of brown fcc C_{60} powder (ultrapure 99.95+%, SES Chemicals Inc.) was hot isostatically pressed for 60 h at 350 °C under 170 MPa of CO_2 to form $C_{60}(CO_2)_x$.[15]

Crystallographic study

Powder neutron diffraction data were collected at $\lambda=1.6663(1)$ Å, over a temperature range 5–293 K, and a step size of 0.1°, on the medium-resolution powder diffractometer (MRPD),[16] using thermal neutrons from the High Flux Australian Reactor (HIFAR) nuclear reactor at the Australian Nuclear Science and Technology Organisation (ANSTO).[17] The sample was housed in a vanadium can and mounted in a closed-cycle helium refrigerator which allowed cooling down to 5 K. Rietveld analysis[18] of the neutron diffraction profiles was performed using the program LHPM (Ref. 19) with a pseudo-Voigt peak shape function and an interpolated background.

RESULTS AND DISCUSSION

Figure 1 shows the powder neutron diffraction profiles of $C_{60}(CO_2)_x$ over the range 293 to 5 K, which indicates a structural transition with the lowering of temperature. A decrease in structural symmetry below ~250 K is reflected in the splitting of diffraction lines, while the growth of peaks in the 2Θ region above ~40° indicates orientational ordering of the molecules in the sample. Examination of Fig. 1 indicates that the structural transition is complete by 150 K. The refined cell parameters and C═O bond lengths of $C_{60}(CO_2)_x$ versus

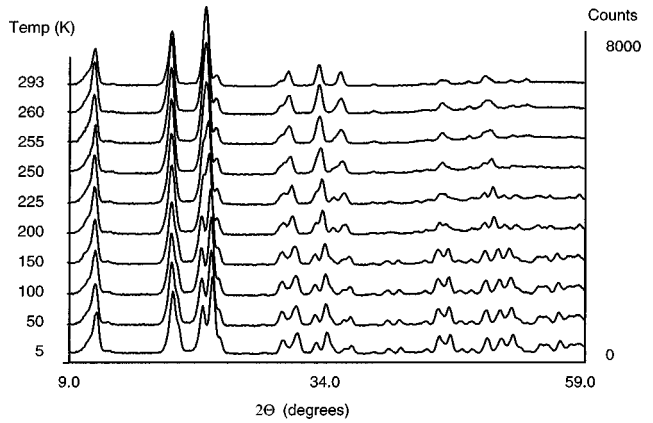

FIG. 1. Powder neutron diffraction profiles of $C_{60}(CO_2)_x$ over the range 293 to 5 K.

TABLE I. Refined cell parameters and C═O bond length for $C_{60}(CO_2)_x$.

Temp. (K)	Space group	a (Å)	b (Å)	c (Å)	β (°)	C═O (Å)
293	$Fm\bar{3}m$	14.224(2)				1.165[a]
260		14.192(4)				
255		14.178(5)				
250		14.158(6)				
150	$P2_1/n$	9.7867(18)	9.7884(17)	14.6150(18)	90.382(11)	1.12(3)
100		9.7621(12)	9.7682(12)	14.6226(14)	90.397(7)	1.07(3)
50		9.7506(11)	9.7559(11)	14.6160(13)	90.383(7)	1.07(2)
5		9.7438(9)	9.7473(9)	14.6121(11)	90.390(6)	1.07(2)

[a]Fixed.

temperature are given in Table I. Structural refinements from the diffraction data collected at 225 and 200 K within the transition region were unsatisfactory using either the high- or the low-temperature structural models; a consequence of insufficient resolution between peaks in the diffraction profile. The nature of the structure of $C_{60}(CO_2)_x$ in the transition region between 150 and 250 K has not been determined, although analysis of our current data suggests the possibility of this being a two-phase region.

High-temperature phase

Figure 2 shows the observed, calculated, and difference powder neutron diffraction profiles for $C_{60}(CO_2)_x$ at 293 K. Rietveld refinement indicates a good fit to the 131 observed reflections using a cubic $[Fm\bar{3}m,\ a=14.224(2)]$ model with CO_2 located in the octahedral interstices between the C_{60} molecules. Refinement of these data indicated no evidence for CO_2 occupying the tetrahedral interstices. The main error in the fit is in the reflections at low 2θ, which can be attributed to hexagonal stacking fault disorders that are generally associated with C_{60}.[20,21] As for previous studies,[1–3,15,20] the C_{60} molecules were modeled using a zero-order spherical Bessel function $j_0=\sin(\kappa R_0)/(\kappa R_0)$ $(\kappa=4\pi\ \sin\theta/\lambda)$. This uniform distribution of the C atoms on the surface of a sphere of radius $R_0=3.54$ Å reflects the orientational disorder produced by the unhindered rotation of the C_{60} molecules and has the additional advantage of reducing the number of structural parameters for the C_{60} molecule to two, R_0, and an isotropic thermal parameter.

Simple geometric arguments suggest that the CO_2 molecules should not be able to freely rotate within the octahedral interstices. Refinements were made with the eight O atoms of the four CO_2 molecules per unit cell disordered over the 32 $f(x,x,x)$ sites, thus aligning the CO_2 along the body diagonal of the cell $[R_P=3.2$, goodness of fit (GOF) $=4.2$, and $R_B=8.9]$ and providing the maximum space between the C_{60} molecules. Attempts to refine the O atoms on other sites in the unit cell did not lead to an improvement in the fit. Refinement of the oxygen position, isotropic thermal parameters, and the occupancy of the CO_2 molecules gave 0.4462(16), 0.08(1) Å^2, and 0.82(2), although these parameters were found to be highly correlated. The C═O bond length of 1.32(2) Å was significantly longer than expected from the literature (1.165 Å) for CO_2 (Ref. 13) and was thought to be an artifact of refinement correlations. In the final refinement the oxygen positions were fixed so as to give the above literature C═O bond length, the thermal parameters were fixed at more physical values and the occupancy was refined and found to be 0.80(2). The fractional coordinates and isotropic thermal parameters for this phase at 293 K are given in Table II.

Low-temperature phase

Figure 3 shows the observed, calculated, and difference neutron diffraction patterns for $C_{60}(CO_2)_x$ at 5 K. Examination of the increased number of reflections in this pattern clearly indicated that this phase could not be refined in the same the $Pa\bar{3}$ space group as the low-temperature forms of

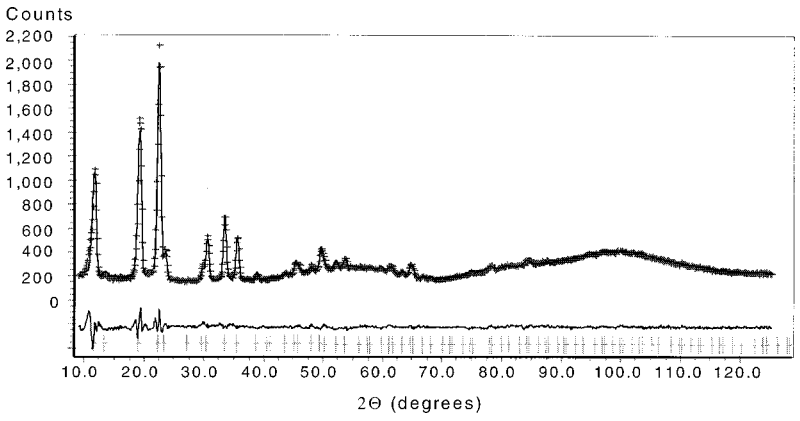

FIG. 2. The observed (+), calculated, and difference (solid lines) powder neutron diffraction profiles for $C_{60}(CO_2)_x$ at 293 K.

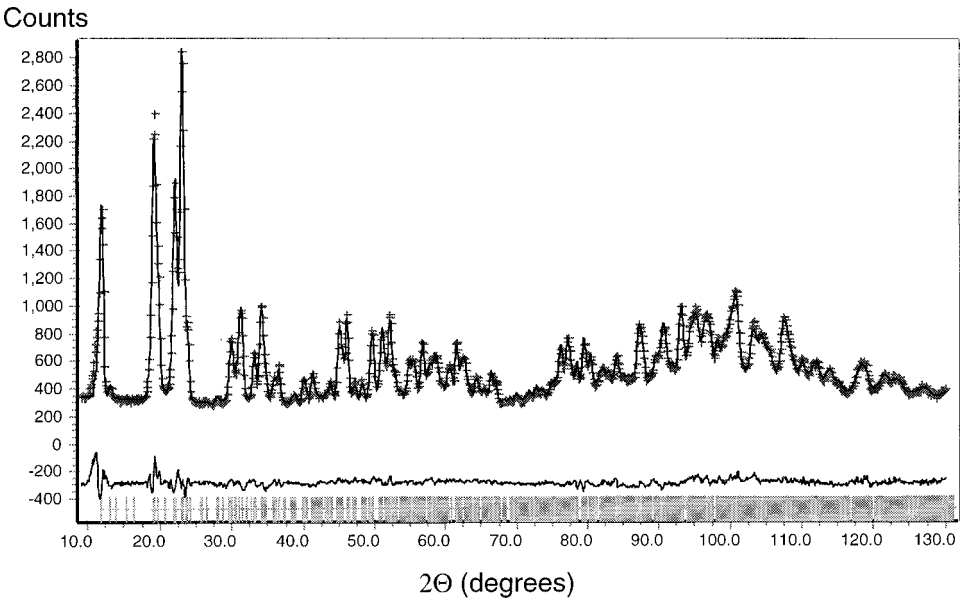

FIG. 3. The observed (+), calculated and difference (solid lines) neutron diffraction patterns for $C_{60}(CO_2)_x$ at 5 K.

the parent compound[8] or the rare gas intercalates R_xC_{60} [R = Ar($x=1.0$),[2] Kr($x=0.84$), Xe($x=0.66$)].[3]

Initial indexing of the reflections suggested a P-centered tetragonal cell with $a\sim 9.76$ Å ($\approx a_{\text{cubic}}/\sqrt{2}$) and $c\sim 14.63$ Å; the new a parameter being generated by a 45° rotation of the crystallographic x and y axes about the z axis. Figure 4 shows the relationship between the $Pa\bar{3}$ cell of the parent compound and the reduced $(a/\sqrt{2})\times(a/\sqrt{2})\times a$ cell of the low-temperature form of $C_{60}(CO_2)_x$. Open circles indicate C_{60} molecules at $z=0$ and shaded circles indicate those at $z=\frac{1}{2}$; while the lines m_1 and m_2 indicate vertical mirror planes in C_{60} and $C_{60}(CO_2)_x$, respectively. Comparison of the lattice parameters of the reduced cell with the equivalent values for the low-temperature form of C_{60} [14.041(1) Å] (Ref. 11) indicate a contraction along the a direction by 2% and an expansion along the c direction by 4% relative to the parent compound. Such an anisotropic variation in cell volume suggested that the CO_2 molecules were oriented in the lattice approximately parallel to the z axis.

Attempts were made to refine the structure in a number of different tetragonal settings. The initial structural model was constructed by translating a cubic model for C_{60} (Ref. 22) into the tetragonal space group $P4_2/mnm$. The fractional coordinates were scaled to reflect the anisotropic cell dimensions relative to the cubic model, so as to ensure spherical C_{60} molecules with radii of 3.54(1) Å. By virtue of the 4 or $\bar{4}$ axis, all of the allowed tetragonal space groups led to a constraint such that the C_{60} molecules must be oriented in the unit cell so as to give rise to a horizontal mirror plane. It was clear from the poor fits (GOF$\sim$200) to the observed data that these tetragonal space groups were unsuitable and that the mirror plane present in the C_{60} molecules did not lie in the ab plane.

The poor fit to these data based on tetragonal space groups suggested further reductions in symmetry. As a starting point for a model in an orthorhombic setting we transformed the low-temperature model for C_{60} from the reported

TABLE II. Fractional atomic coordinates and equivalent isotropic thermal parameters (B_{eq}) (Å$^2\times$100) for $C_{60}(CO_2)_x$ at 293 K, with estimated standard deviations in parentheses.

Atom	x	y	z	B_{eq}[a] (Å$^2\times$100)
C1	0	0	0	1.0(1)[b]
C[c]	0.5	0.5	0.5	5.0
O[c]	0.452 88[d]	0.452 88	0.452 88	5.0

[a]$B_{\text{eq}} = 8/3\pi^2[U_{11}(aa^*)^2 + U_{22}(bb^*)^2 + U_{33}(cc^*)^2 + 2U_{12}aa^*bb^*\cos\gamma + 2U_{13}aa^*cc^*\cos\beta + 2U_{33}bb^*cc^*\cos\alpha]$.

[b]The thermal parameter of C1 relates to freely rotating C_{60} molecules.

[c]Occupancy of $CO_2 = 0.80(2)$.

[d]Calculated position based on a 1.165 Å bond length.

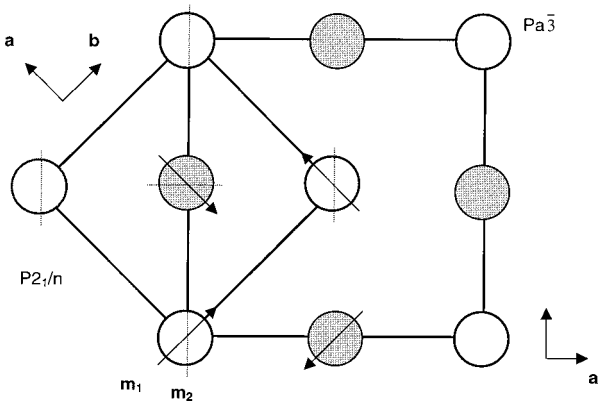

FIG. 4. The relationship between the $Pa\bar{3}$ cell of the C_{60} and the $(a/\sqrt{2})\times(a/\sqrt{2})\times a$ cell of the low-temperature form of $C_{60}(CO_2)_x$. Open circles indicate C_{60} molecules at $z=0$ and shaded circles indicate those at $z=\frac{1}{2}$. m_1 (solid) and m_2 (dashed) indicate vertical mirror planes in C_{60} and $C_{60}(CO_2)_x$, respectively. Arrows denote the sense of tilting of the molecule along the $\langle\pm1\pm1\pm1\rangle$ directions (see text).

$Pa\bar{3}$ space group[8] to the *Pbca* space group. Refinements were carried out after rotations of the C_{60} molecule with respect to the unit cell axes in 5° or 10° steps. No satisfactory solutions were obtained, although the series of rotations that minimized the goodness of fit (GOF~100) saw a mirror plane of the C_{60} molecules aligned approximately normal to the $\langle 110 \rangle$ direction.

Lowering of the symmetry yet further to a monoclinic ($P2_1/n$) space group was necessary in order to generate the correct relationship between the two symmetry-related C_{60} molecules in the unit cell: $(x,y,z) \rightarrow (x+\frac{1}{2},\bar{y}+\frac{1}{2},z+\frac{1}{2})$. Further small rotations (1°) of the C_{60} molecules yielded a structure [$a=9.7438(9)$ Å, $b=9.7473(9)$ Å, $c=14.6121(11)$ Å, $\beta=90.390(6)°$] that gave a good fit ($R_P=3.1\%$, GOF=6.8, $R_B=5.4\%$) to the observed data. In order to avoid correlations between CO_2 thermal parameters and occupancy the latter was fixed at the value of 0.80 as determined from the room-temperature profile. The refined fractional coordinates and isotropic thermal parameters for $C_{60}(CO_2)_x$ are listed in Table III, while the nearest-neighbor intermolecular contacts between C_{60} and CO_2 molecules are given in Table IV. The refined unit cell is shown in Fig. 5(a), while the orientation of the CO_2 molecules with respect to the *c* axis is highlighted in Fig. 5(b). Note that the oxygen atoms are adjacent to the pentagonal faces of the adjacent C_{60} molecules.

In order to confirm the monoclinic cell of the low-temperature form of $C_{60}(CO_2)_x$, a diffraction profile was collected at a longer neutron wavelength [$\lambda=1.9905(1)$ Å]. The structure was refined in the monoclinic setting as well as an orthorhombic setting ($P2_1/n$ with β fixed at 90°). The monoclinic setting gave a superior fit to the data (mono: $R_P=4.1\%$, GOF=4.6%; ortho: $R_P=5.6\%$, GOF=8.4%) and it was clear from these refinements that some peak splittings were present which could not be explained using orthorhombic symmetry.

The orientation of the C_{60} molecules with respect to one another in the low-temperature form of $C_{60}(CO_2)_x$ are substantially different to those observed in the low-temperature form of the parent compound.[11] In the case of pure C_{60}, the molecule centered at (0,0,0) has hexagonal faces which are normal to the $\langle 111 \rangle$ direction with pentagonal faces aligned essentially normal to the $\langle 110 \rangle$ direction [Fig. 6(a)]. The orientation places one of the molecule's three mutually orthogonal mirror planes vertical and perpendicular to the $\langle 1\bar{1}0 \rangle$ direction [Fig. 6(b) and m_1 in Fig. 4].[11,23] The orientational ordering in pure C_{60} is dominated by van der Waals bonding and electrostatic repulsion so as to have the most electron-poor regions (the pentagonal faces) facing the most electron-rich regions (the interpentagon 6:6 bonds) of adjacent C_{60} molecules [indicated by gray shading in Fig. 6(b)]. The nearest-neighbor molecules at $(\frac{1}{2},0,\frac{1}{2})$, $(0,\frac{1}{2},\frac{1}{2})$, and $(\frac{1}{2},\frac{1}{2},0)$ have hexagonal faces oriented normal to $\langle \bar{1}11 \rangle$, $\langle 1\bar{1}1 \rangle$, and $\langle \bar{1}\bar{1}1 \rangle$, respectively. This is illustrated in Fig. 4 by solid arrows, where the sense of the arrows indicates a tilting of this axis above the plane of the page.

The orientation of C_{60} molecules in $C_{60}(CO_2)_x$ is determined by van der Waals and electrostatic interactions between both the intercalated CO_2 molecules and the neighboring C_{60} molecules. Figure 4 shows that the vertical mirror planes (indicated by dashed lines m_2) in $C_{60}(CO_2)_x$ have been rotated by approximately 45° relative to the vertical mirror planes (m_1) in C_{60}. As a consequence, both m_1 and m_2 retain similar orientations with respect to their structural axes. Comparison of these mirror planes in C_{60} [Fig. 6(b)]

TABLE III. Fractional atomic coordinates and equivalent isotropic thermal parameters (B_{eq}) (Å$^2\times$100) for $C_{60}(CO_2)_x$ at 5 K, with estimated standard deviations in parentheses.

Atom	*x*	*y*	*z*	B_{eq}[a] (Å$^2\times$100)
C1	0.0873(1)	−0.3502(1)	0.0270(1)	1.0(1)
C2	0.0293(1)	0.3503(3)	−0.0599(1)	1.0(1)
C3	0.2182(1)	−0.2842(3)	0.0425(1)	1.0(1)
C4	−0.1169(1)	−0.3259(4)	−0.0714(1)	1.0(1)
C5	0.0016(1)	−0.3258(4)	0.1072(1)	1.0(1)
C6	0.2238(2)	−0.2231(1)	−0.1191(2)	1.0(1)
C7	0.0985(2)	−0.2862(1)	−0.1337(2)	1.0(1)
C8	0.2844(3)	−0.2223(1)	−0.0287(3)	1.0(1)
C9	−0.1995(2)	−0.3025(1)	0.0061(4)	1.0(1)
C10	−0.1393(3)	−0.3022(1)	0.0962(3)	1.0(1)
C11	0.2088(3)	0.0123(2)	0.1992(4)	1.0(1)
C12	0.0811(2)	−0.0125(1)	0.2368(3)	1.0(1)
C13	0.2764(2)	−0.0930(1)	0.1462(3)	1.0(1)
C14	−0.0245(1)	−0.0929(1)	0.2336(1)	1.0(1)
C15	0.2378(1)	0.1444(3)	0.1564(1)	1.0(1)
C16	0.0814(1)	−0.2424(3)	0.1732(1)	1.0(1)
C17	0.0169(1)	−0.1414(4)	0.2237(1)	1.0(1)
C18	0.2142(1)	−0.2169(4)	0.1335(1)	1.0(1)
C19	0.0038(2)	0.2205(1)	0.1924(2)	1.0(1)
C20	0.1362(2)	0.2462(1)	0.1532(2)	1.0(1)
C21	0.3319(3)	−0.0071(1)	−0.0974(3)	1.0(1)
C22	0.3087(2)	0.1326(1)	−0.0910(4)	1.0(1)
C23	0.3521(3)	−0.0878(1)	−0.0151(3)	1.0(1)
C24	0.2057(3)	0.1977(2)	−0.1490(4)	1.0(1)
C25	0.2533(2)	−0.0893(1)	−0.1625(3)	1.0(1)
C26	0.3245(2)	0.1197(1)	0.0751(3)	1.0(1)
C27	0.3052(2)	0.1966(1)	−0.0038(3)	1.0(1)
C28	0.3483(2)	−0.0260(1)	0.0688(3)	1.0(1)
C29	0.1299(2)	0.1182(1)	−0.2120(3)	1.0(1)
C30	0.1540(2)	−0.0268(1)	−0.2185(3)	1.0(1)
C	0	0	0.5	2.1(5)
O	0.0393(2)	0.0083(1)	0.5703(3)	2.2(5)

[a] $B_{eq}=8/3\pi^2[U_{11}(aa^*)^2+U_{22}(bb^*)^2+U_{33}(cc^*)^2+2U_{12}aa^*bb^*\cos\gamma+2U_{13}aa^*cc^*\cos\beta+2U_{33}bb^*cc^*\cos\alpha]$.

TABLE IV. Intermolecular distances (Å) in $C_{60}(CO_2)_x$ at 5 K.

		$C(C_{60})$-O (*z* axis)			
C14-O	3.03(1)	C12-O	3.06(1)	C30-O	3.30(1)
C17-O	3.33(1)	C29-O	3.48(1)		
		$C(C_{60})$-O ($\langle 110 \rangle$)			
C8-O	3.22(1)	C9-O	3.39(1)	C27-O	3.53(1)
C3-O	3.55(1)	C6-O	3.58(1)		
		$C(C_{60})$-$C(CO_2)$ ($\langle 110 \rangle$)			
C8-C	3.45(1)	C9-C	3.51(1)	C3-C	3.52(1)
C27-C	3.52(1)				

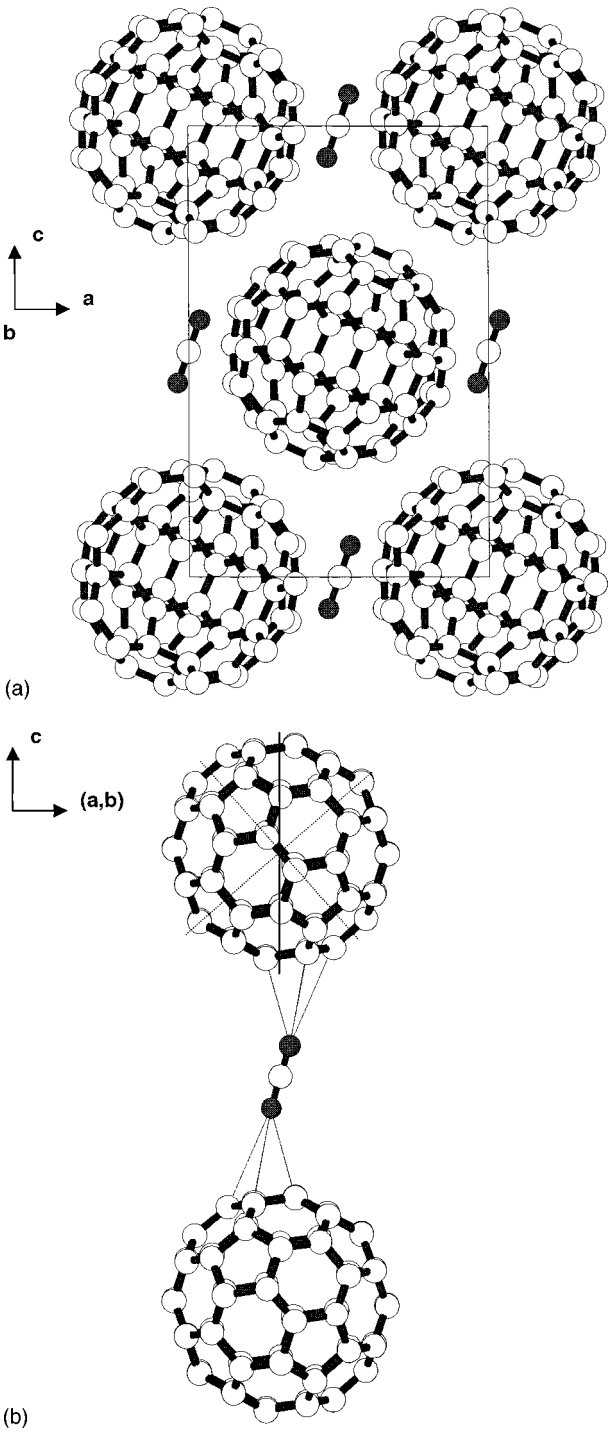

FIG. 5. The low-temperature structure of $C_{60}(CO_2)_x$: (a) Viewed along the *b* axis; (b) viewed along the $\langle 110 \rangle$ direction, showing intermolecular contacts between C_{60} and CO_2. The mirror plane m_2 is in the plane of the page and the two mutually orthogonal mirror planes of the C_{60} molecule are represented by dashed lines.

and $C_{60}(CO_2)_x$ [Fig. 5(b)] indicate that their orientations also differ by a ~15° rotation about $\langle 1\bar{1}0 \rangle$.

Examination of the cell parameters of C_{60} and $C_{60}(CO_2)_x$ indicates a contraction along the *a* and *b* directions and an expansion along the *c* direction of the latter. The low-temperature form of C_{60} is a highly frustrated system with van der Waals and electrostatic interactions in three dimensions. Intercalation of CO_2 into the C_{60} lattice has effectively forced the C_{60} molecules apart along the *z* axis, allowing the lattice to relax in the *xy* plane, leading to a pseudo-two-dimensional structure. The C═O bond length in the low-temperature form of $C_{60}(CO_2)_x$ was refined to a value of 1.07(2) Å; an 8% reduction in length compared to the room-temperature value. When this is related to the 4% reduction in volume of the unit cell of $C_{60}(CO_2)_x$ between room temperature and 5 K, the strength of the compressive forces acting axially on the CO_2 molecules becomes apparent.

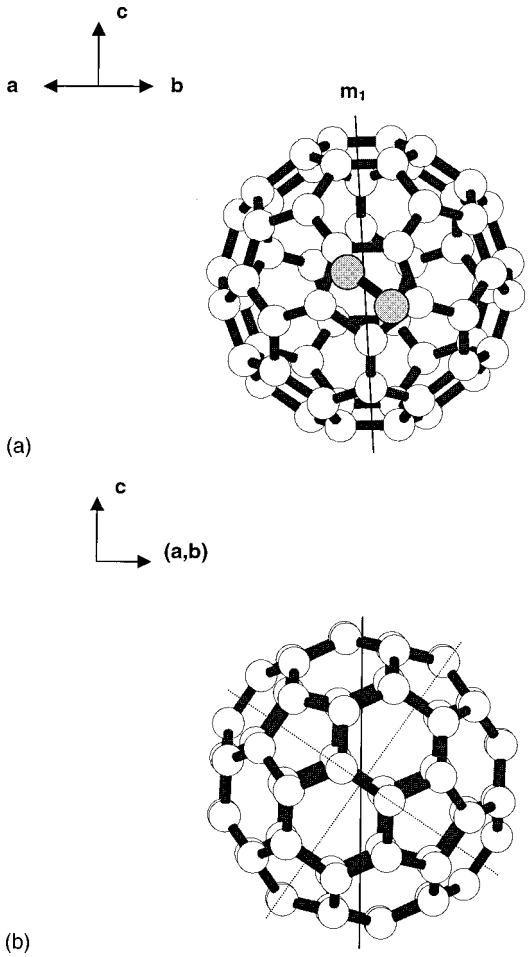

FIG. 6. The orientation of molecules in the low-temperature form of pure C_{60}: (a) Viewed along the $\langle 110 \rangle$ direction; the shaded atoms are those of the interpentagonal 6:6 bond in the nearest-neighbor C_{60} molecule; (b) viewed along the $\langle 1\bar{1}0 \rangle$ direction. The mirror plane m_1 is in the plane of the page and the two mutually orthogonal mirror planes of the C_{60} molecule are represented by dashed lines.

The orientation of the CO_2 molecules with respect to the C_{60} molecules was also refined in the final structural model. The CO_2 molecules were found to be oriented such that the C═O bond was tilted approximately 21° from the *bc* plane [Fig. 5(a)] and ~5° from the *ac* plane. The effect of this tilting is to place the O atoms adjacent to a pentagonal face of the nearest-neighbor C_{60} molecule along the *z* axis. Intermolecular contact distances between the O atom of the CO_2 molecules and the C atoms of the adjacent pentagonal face [Fig. 5(b)] range from 3.03(1) to 3.48(1) Å (Table IV). Electrostatic forces can also be envisaged between the CO_2 and C_{60} molecules where the electron-poor pentagonal faces of

the C_{60} face the electron-rich oxygen atoms of the CO_2 molecules. The lowering of crystal symmetry to monoclinic in the low-temperature form of $C_{60}(CO_2)_x$ can thus be seen as the net result of the interplay between van der Waals and electrostatic forces, leading also to the tilting of CO_2 molecules away from the vertical.

The combination of van der Waals and electrostatic interactions observed between molecules in $C_{60}(CO_2)_x$ at low temperature has also been reported by van Smaalen and coworkers for $(CO)_xC_{60}$ ($x=0.67$).[10] In this instance, as in the case of the rare gas intercalated compounds,[2,3] the cubic close packing of the C_{60} molecules was not disturbed by the presence of the intercalate and the relative orientations of the C_{60} molecules were found to be the same as for the parent compound. The intermolecular interactions reported for $(CO)_xC_{60}$ do differ slightly from those observed in our study. The results of their structural refinement using synchrotron x-ray diffraction data led them to conclude that the CO molecule was oriented such that the C atom, being the negative component of the dipole, was facing its nearest-neighbor C_{60} molecule and positioned above an electron-poor 6:5 bond. The distances between the C atom of the CO molecule and the two atoms of the adjacent 6:5 bond of the C_{60} molecule [2.39(5) and 2.55(4) Å] suggest a significantly stronger intermolecular interaction than is the case for $C_{60}(CO_2)_x$. This is a consequence of the fact that the CO_2 molecule interacts symmetrically and most strongly with the two axial C_{60} molecules of the distorted octahedron surrounding it, while the CO molecule interacts primarily with only one of the six C_{60} molecules of a regular octahedron.

In conclusion, we have determined the structure of the intercalate compound $C_{60}(CO_2)_x$ at temperatures between 5 K and room temperature using powder neutron diffraction and Rietveld techniques. A structural transition is observed between a high-temperature fcc phase and a low-temperature monoclinic phase in which the C_{60} and CO_2 molecules become orientationally ordered; a consequence of electrostatic and van der Waals interactions. Expansion of the low-temperature structure along the *c* axis due to vertically oriented CO_2 leads to a reduction in the three-dimensional frustration observed in other C_{60}-based systems. The structure of this compound in the transition region between 150 and 250 K has not been adequately determined and is currently the subject of a high-resolution synchrotron diffraction study.

*Author to whom correspondence should be addressed.

[1] G. E. Gadd, M. James, S. Moricca, P. J. Evans, and R. L. Davis, Fullerene Sci. Technol. **4**, 853 (1996).

[2] G. E. Gadd, S. J. Kennedy, S. Moricca, C. J. Howard, M. M. Elcombe, P. J. Evans, and M. James, Phys. Rev. B **55**, 14 794 (1997).

[3] G. E. Gadd, S. Moricca, S. J. Kennedy, M. M. Elcombe, P. J. Evans, M. Blackford, D. Cassidy, C. J. Howard, P. Prasad, J. V. Hanna, A. Burchwood, and D. Levy, J. Phys. Chem. Solids **58**, 1823 (1997).

[4] J. E. Schirber, G. H. Kwei, J. D. Jorgensen, R. L. Hitterman, and B. Morosin, Phys. Rev. B **51**, 12 014 (1995).

[5] B. Morosin, J. D. Jorgensen, Simine Short, G. H. Kwei, and J. E. Schirber, Phys. Rev. B **53**, 1675 (1996).

[6] R. A. Assink, J. E. Schirber, D. A. Loy, B. Morosin, and G. A. Carlson, J. Mater. Res. **7**, 2136 (1992).

[7] A. Dworkin, H. Szwarc, and R. Ceolin, Europhys. Lett. **22**, 35 (1993).

[8] H. Werner, M. Wohlers, D. Bublak, T. Belz, W. Bensch, and R. Schogl, in *Electronic Properties of Fullerenes*, edited by H. Kuzmany *et al.*, Springer Series in Solid-State Sciences Vol. 117 (Springer, Berlin, 1993), p. 16.

[9] W. Bensch, H. Werner, H. Bartl, and R. Schlögl, J. Chem. Soc., Faraday Trans. **90**, 2791 (1994).

[10] S. van Smaalen, R. Dinnebier, I. Holleman, G. von Helden, and G. Meijer, Phys. Rev. B **57**, 6321 (1998).

[11] W. I. F. David, R. M. Ibberson, J. C. Mattewman, K. Prassides, T. J. Dennis, J. P. Hare, H. W. Kroto, R. Taylor, and D. R. M. Walton, Nature (London) **353**, 147 (1991).

[12] M. J. Rosseinsky, Mater. Chem. Phys. **5**, 1497 (1995).

[13] G. Herzberg, *Molecular Spectra and Molecular Structure, II Infrared and Raman Spectra of Polyatomic Molecules* (Van Nostrand Reinhold, New York, 1945), Vol. II, p. 398.

[14] A. Bondi, J. Phys. Chem. **68**, 441 (1964).

[15] G. E. Gadd, M. James, S. Moricca, D. Cassidy, P. J. Evans, B. Collins, and R. S. Armstrong, J. Phys. Chem. Solids (to be published).

[16] C. J. Howard and S. J. Kennedy, Mater. Forum **18**, 155 (1994).

[17] S. J. Kennedy, Adv. X-Ray Anal. **38**, 35 (1995).

[18] H. M. Rietveld, J. Appl. Crystallogr. **2**, 65 (1969).

[19] C. J. Howard and B. A. Hunter, *A Computer Program for Rietveld Analysis of X-ray and Neutron Powder Diffraction Patterns* (Australian Nuclear Science and Technology Organisation, Menai, 1997).

[20] G. B. M. Vaughan, Y. Chabre, and D. Dubois, Europhys. Lett. **31**, 525 (1995).

[21] J. E. Fischer, P. A. Heiney, D. E. Luzzi, and D. E. Cox, *ACS Symposium Series* (American Chemical Society, Washington DC, 1992), Vol. 481, Chap. 4.

[22] P. W. Stephens, L. Mihaly, P. L. Lee, R. L. Whetten, S.-M. Huang, R. Kaner, F. Deiderich, and K. Holczer, Nature (London) **351**, 632 (1991).

[23] W. I. F. David, R. M. Ibberson, T. J. S. Dennis, J. P. Hare, and K. Prassides, Europhys. Lett. **18**, 219 (1992).